Al Falou, H. et al. (2013). Inelastic scattering of 9Li and excitation mechanism of its first excited state. Physics Letters B, 721: 224-228
http://dx.doi.org/10.1016/j.physletb.2013.03.018

Inelastic scattering of ^{9}Li and excitation mechanism of its first excited state

H. Al Falou, R. Kanungo, C. Andreoiu, D.S. Cross, B. Davids, M. Djongolov, A.T. Gallant, N. Galinski, D. Howell, R. Kshetri, D. Niamir, J.N. Orce, A.C. Shotter, S. Sjue, I. Tanihata, I.J. Thompson, S. Triambak, M. Uchida, P. Walden and R.B. Wiringa

Abstract

The first measurement of inelastic scattering of ^{9}Li from deuterons at the ISAC facility is reported. The measured angular distribution for the first excited state confirms the nature of excitation to be an E2 transition. The quadrupole deformation parameter is extracted from an analysis of the angular distribution.

The neutron-rich nuclei close to the drip-line are subject of great interest due to the variance in their properties from our conventional knowledge of nuclear structure. The neutron halo in ^{11}Li [1] continues to be an intriguing quantum system whose complete understanding, from a microscopic view, is still an outstanding problem. It is important to understand how the two fragile halo neutrons are correlated and bound to the ^{9}Li core. It has been discussed that the bare nucleon–nucleon pairing interaction is not sufficient to bind the halo neutrons. The ^{9}Li core is suggested to play a more dynamic role in providing the glue to bind the halo neutrons through quadrupole vibrational phonon exchange [2]. Knowledge on the properties of ^{9}Li is therefore important for a complete understanding of the structure of the neutron-rich lithium isotopes. The two-neutron transfer reaction from ^{11}Li, interestingly, observed some fraction of the ^{9}Li core in its first excited state [3]. The angular distribution of this reaction channel could be interpreted in the framework of nuclear field theory [4] using a wavefunction of ^{11}Li that contains a component with the ^{9}Li core in its first excited state. However, no experimental information exists on the nature of excitation of ^{9}Li to its first excited state.

The neutron-rich *p*-shell nuclei also offer the scope of investigation using *ab initio* theories, which have significantly advanced in recent times. This makes it important to have experimental information on their structure and excitation mechanisms, that serve as testing grounds for the newly developed models.

In this Letter we report the first measurement of inelastic scattering of ^{9}Li from deuterons. The observation shows evidence of a quadrupole collective excitation component for the first excited state in ^{9}Li at 2.69 MeV.

The early measurements of two-neutron transfer in ^{7}Li(t, p) ^{9}Li showed the first excited state of ^{9}Li [5,6] to be located at excitation energy (E_{ex}) of 2.691 ± 0.005 MeV. The next excited state was observed at 4.296 ± 0.015 MeV [7]. The ^{11}B(^{6}Li, ^{8}B)^{9}Li reaction [8] showed a strong population of the ^{9}Li ground state which was consistent with predicted two-proton transition strengths. A weaker population of excited states at 2.69, 4.31 and 6.41 MeV was also seen. The observed excitation energies are in good agreement with shell model predictions of Poppelier et al. [9].

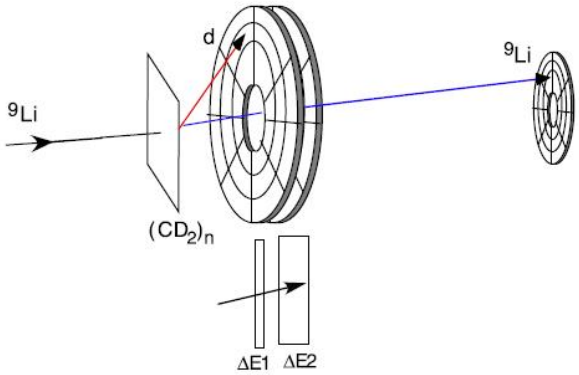

Fig. 1. Schematic view of the experimental setup.

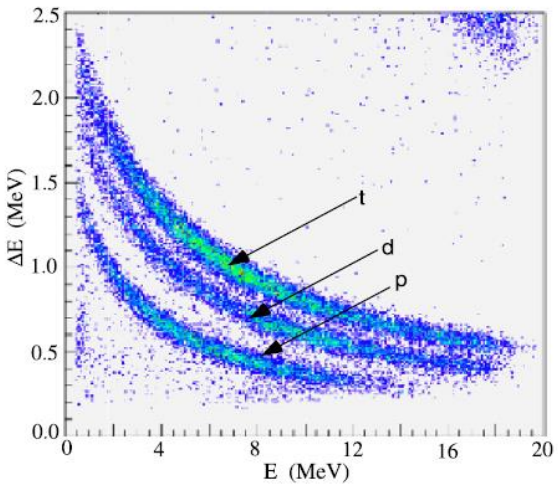

Fig. 2. Particle identification by ΔE–E correlation.

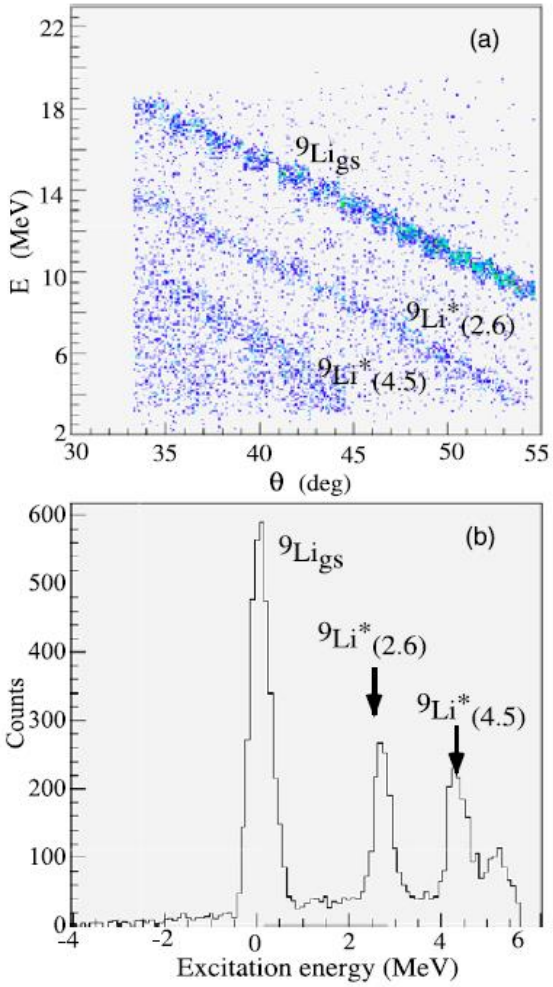

Fig. 3. (a) The kinematic loci from the deuterons detected in the YY1 detector array. (b) The Q-value spectrum of d(^{9}Li, d) reactions.

The spin of the first excited state predicted by the $(0 + 1)\hbar\omega$ model space in this shell model calculation [9] is $1/2^-$, while a $5/2^-$ spin is predicted with a $(0 + 2)\hbar\omega$ model space.

Ab initio calculations using either the Green's function Monte Carlo method [10] or the no-core shell model [11] predict a $1/2^-$ first excited state for ^{9}Li (see Table I of Ref. [12]). In both cases, the excitation energies are in better agreement with observations if a realistic three-nucleon potential is added to the underlying two-nucleon force.

The one-neutron transfer reaction on ^{8}Li [12] was found to populate the excited states at 2.69, 4.31, 5.38 and 6.43 MeV in ^{9}Li. A DWBA analysis of the angular distribution of the 2.69 MeV first excited state yielded a spectroscopic factor of 0.73(15). This value in general is higher than theoretical predictions and agrees only at the lower end of the uncertainty with the value of 0.52 predicted by the Variational Monte Carlo [10] and the no-core shell model [11] predictions.

To investigate the nature of the first excited state in ^{9}Li, an inelastic scattering experiment was performed at the ISAC-II facility at TRIUMF. The schematic view of

the setup is shown in Fig. 1. The radioactive beam of ^{9}Li with an average intensity of 5×10^{4}/sec and energy of 5 A MeV was inelastically scattered off a deuterated polyethylene foil $(CD_2)_n$ target of thickness 490 μg/cm^2. Annular arrays of segmented silicon strip detectors (YY1), arranged in two layers, detected the scattered deuterons and other light target-like charged particles from the reaction. The layers were arranged as energy loss (ΔE) followed by the stopping detector (E) configuration. This enabled an identification of the reaction channel from a ΔE–E correlation (Fig. 2). The ΔE layer covered laboratory angles from 35° to 60°. Another annular detector, S2, placed further downstream covering laboratory angles from 2.6° to 8.0° was used to detect the heavy projectile-like residue.

The kinematic loci of the scattered deuterons from elastic and inelastic scattering are shown in Fig. 3(a). The $^{9}Li_{gs}$, ^{9}Li*(2.69 MeV) first excited state and the ^{9}Li*(4.5 MeV) second excited states were populated. The discrete band-like structures seen in the loci are due to segmentation of the detectors. The corresponding Q-value spectrum is shown in Fig. 3(b).

The inclusive spectrum of the S2 detector is shown in Fig. 4(a). The elastic scattering from the carbon in the $(CD)_2$ foil target is observed as the intense nearly horizontal band. In the very small laboratory angles Rutherford scattering on carbon dominates, whose cross section allows a determination of the beam intensity and the absolute normalization of the data. The ^{9}Li elastically scattered from the deuterons appears as the curved bright band in Fig. 4(a). This corresponds to the forward center of mass scattering angles. The band observed at energies higher than the Rutherford scattering originates from the d(^{9}Li, ^{8}Li)t reaction. The kinematic correlation of the S2 detector in a coincidence condition with the E detector allowed the detection of forward center of mass angle events for the ^{9}Li first excited state (Fig. 4(b)).

The angular distribution for the elastic scattering of ^{9}Li from deuterons is shown in Fig. 5. The uncertainties include a 5% systematic error arising from the target thickness uncertainty. The inelastic scattering data have been interpreted in a zero-range one-step distorted wave Born approximation framework using the computer code DWUCK4 [13] as well as the coupled channels framework using FRESCO [14].

The optical potential parameters for the ^{9}Li + d interaction were determined from a best fit to these data by a χ^2 minimization search (solid line).

Table 1
Optical potential parameters.

Set	V_0 (MeV)	r_0 (fm)	a_0 (fm)	W_v (MeV)	r_v (fm)	a_v (fm)	W_d (MeV)	r_d (fm)	a_d (fm)	V_{so} (MeV)	r_{so} (fm)	a_{so} (fm)
set-1	43.023	2.042	0.627	4.067	1.400	0.800	18.804	1.907	0.189	4.500	1.200	0.700
set-2	35.597	2.327	0.524				24.573	2.020	0.246	4.500	1.200	0.700
set-3	25.530	2.765	0.303	0.117	2.277	0.193	36.150	2.277	0.193	4.500	1.200	0.700

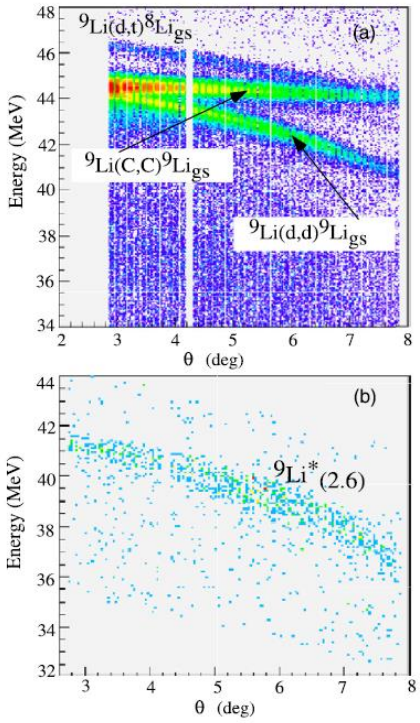

Fig. 4. The kinematic loci from the lithium detected in the S2 detector array. (a) Inclusive spectrum. The identified kinematic loci from the different reactions are labeled in the figure. (b) Spectrum in coincidence with the ΔE YY1 array for the energy region relevant for the first excited state of ^{9}Li.

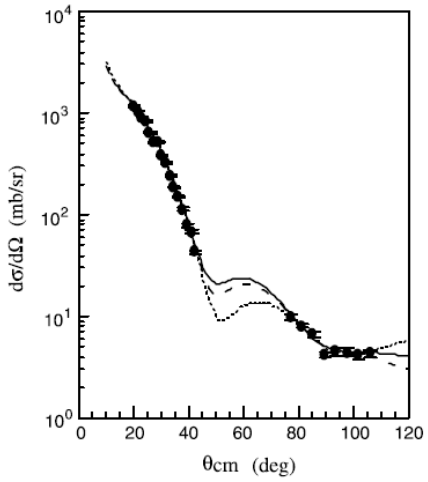

Fig. 5. The angular distribution data for ^{9}Li + d elastic scattering at $E_{lab} = 5A$ MeV. The solid line shows calculations with the set-1 optical potential parameters from Table 1 using the code DWUCK4. The dashed (dotted) lines are coupled channel calculations, with potential set-2 (set-3).

The potential consisted of real, imaginary and spin–orbit interactions of a Woods–Saxon form and is defined as [13]

$$V(r) = -V_0 f(x_0) - iW_v f(x_v) + 4W_d \frac{df(x_d)}{dx_d} - V_{so}\left(\frac{\hbar}{m_\pi c}\right)^2 \frac{1}{r}\frac{df(x_{so})}{dr}(\vec{L}\cdot\vec{s}) \quad (1)$$

where

$f(x_i) = 1/[1 + \exp(x_i)]$,

$x_i = (r - r_i A^{1/3})/a_i, \quad i = 0, v, d$ and so.

The potential parameters found from this best fit are listed as set-1 in Table 1. The potential was found to yield identical fit to the data using two other codes PTOLEMY and FRESCO. These optical potentials were then used for calculating the angular distributions for the inelastic scattering channel.

We have investigated various possible excitation schemes to interpret the angular distribution of excitation to the first excited state of ^{9}Li that is described below. The *ab initio* calculations predict the first excited state of ^{9}Li to have a spin of $1/2^{-}$. The possible modes of excitation of this state from the $3/2^{-}$ ground state of ^{9}Li is therefore either a spin-flip M1 or an E2 quadrupole excitation.

The quadrupole E2 excitation cross section is calculated using a collective form factor [13]. The Woods–Saxon potential in the form factor was taken to be the same as the set-1 real and imaginary parameters. The solid line in Fig. 6(a) shows the result normalized using the relation [13]

$$\frac{d\sigma_{ex}}{d\Omega} = \beta_l^2 \langle J_i l K 0 | J_f K \rangle^2 \frac{d\sigma_{\mathrm{DWUCK4}}}{d\Omega} \qquad (2)$$

where βl is the quadrupole deformation parameter, $J i$ and $J f$ are the spins of the initial (ground) and final (excited) states respec- tively, of the nucleus. $K = 1/2$ for this case. The parameters βl $(l = 2)$ were obtained by normalizing the calculated angular distribution to the data at forward center of mass scattering angles ($\theta_{cm} < 40^{\circ}$). The angular distribution assuming an E2 excitation clearly resembles the trend of the experimental data. The value of β_2 extracted was 0.414 ± 0.023 (Table 2).

Using the same parameter set (set-1) the DWBA calculation performed using the code FRESCO is shown by the dashed-dotted line in Fig. 6(a). The collective form factors used in FRESCO is of the same form as used in DWUCK4. In FRESCO, the deformation is ex- pressed using the deformation length (δ_2). It is obtained from a best fit to the forward angle region ($\theta_{cm} < 40^{\circ}$) that yields value of 1.846 fm. This can be related to the deformation parameter β_2 by the relation $\beta_2 = \delta_2/(r_0 A^{1/3})$. This leads to a deformation parameter of 0.434, in agreement with that obtained using the code DWUCK4.

The deviations of both the DWBA results from the data at the very backward center of mass angles may arise from a more complex multi-step reaction mechanism which would become important for such large momentum transfers. Coupled channel calculations were therefore performed using the code FRESCO in the framework of the rotational model to investigate this.

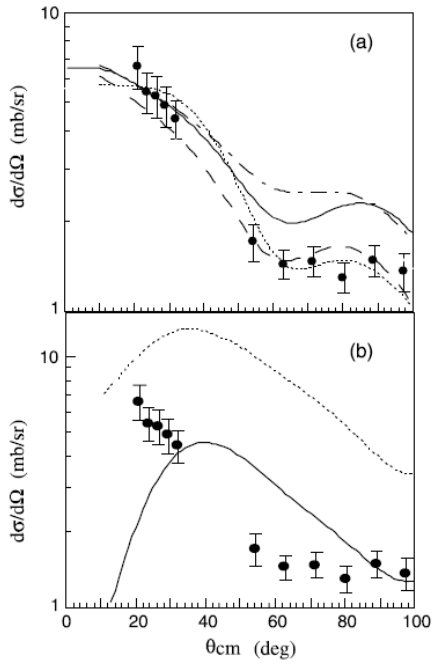

Fig. 6. The angular distribution data for ^{9}Li + d inelastic scattering to the first excited state of ^{9}Li at $E_{lab} = 5A$ MeV. (a) The solid curve (dashed-dotted) is a DWBA calculation with an E2 collective form factor using DWUCK4 (FRESCO) with potential set-1. The dashed (dotted) lines are coupled channel calculations, with potential set-2 (set-3). (b) The curves are DWBA calculations for an M1 excitation form factor. The solid (dotted) curve is for neutron (proton) excitation.

Table 2
Deformation parameters.

	δ_2	β_2
Inelastic DWBA (set-1)	1.846 ± 0.01	0.434 ± 0.01
Inelastic CC (set-2)	1.883 ± 0.092	0.389 ± 0.092
Inelastic CC (set-3)	1.941 ± 0.064	0.337 ± 0.064
Quadrupole moment		0.805 ± 0.005

Since the ground state of ^{9}Li is $3/2^{-}$ and its excited state has a lower spin of $1/2^{-}$, this would correspond to an intra-band transition in a rotational model framework. This is a $K = 1/2$ rotational band. Because of the deformation of ^{9}Li, the coupled channel results change the predicted elastic scattering, and it then becomes necessary to fit the elastic and inelastic cross sections simultaneously. The present data allow this to be done, and furthermore remove the need for model assumptions about the shape of the elastic polarization potential arising from the coupling. A coupled channel fit was therefore performed. All components of the bare optical potential were assumed to have the same deformation length δ_2, which was also a search variable.

Two different fits are shown in Fig. 6(a) corresponding to two potential parameter sets, set-2 (dashed line) and set-3 (dotted line). As seen from Fig. 6 the potential set-2 tends to show an improved fit for the larger center of mass angle data, where multi-step reaction mechanism effects are stronger. Since the forward angle data is less sensitive to higher order processes in the reaction mechanism, we performed a calculation to fit the forward angle region better. The set-3 potentials were obtained by placing a stronger weight in the fitting, through reducing uncertainty for the first point of the angular distribution. The coupled channel calculations show satisfactory

simultaneous reproduction of the forward and backward angle distribution. The elastic scattering angular distribution is well reproduced and the differences between the different sets is visible only in the region of $\theta_{cm} \sim 40^{\circ}-70^{\circ}$ (Fig. 5). The deformation lengths for set-2 and set-3 were found to be 1.883 fm and 1.941 fm respectively. The deformation parameter, β_2 , extracted using the r_0 from Table 1 yields values of 0.389 and 0.337 for set-2 and set-3 respectively (Table 2).

The M1 spin-flip excitation is characterized by an orbital angular momentum transfer of $t..L = 0$ and spin transfer $t..S = 1$. We considered the microscopic form factor model in DWUCK4 for describing the M1 excitation. This model considers the potential between the deuteron and any one of the nucleons in the ^{9}Li nucleus. The form factor was calculated considering a Yukawa potential $V(r) = V_0/(\mu r) \exp(-\mu r)$ [13]. The parameters for the strength V_0 is assumed to be 20 MeV and the inverse range μ is taken as 0.7 fm. A variation of these parameters changes the cross section magnitudes greatly but does not change shape of the angu- lar distribution appreciably. As an example we mention that if the strength V_0 is 40 MeV then the cross section is a factor of four larger. An increase in μ by 0.1 fm leads to a cross section that is about factor of two lower in the region of $\theta_{cm} > 40^{\circ}$ but is higher at the smaller θ_{cm} values.

In this microscopic description the excitation can be considered either as a proton excitation or a neutron excitation. To describe a proton excitation we consider the bound state of ^{8}He + a pro- ton in the $1p_{3/2}$ orbital. In the ground state the binding energy of the single particle is $S_p = -13.93$ MeV while that in the excited state is $S_p - E^*$, with E^* being the excitation energy of the state.

The calculated curve without any further normalization is shown in Fig. 6(b) by the dotted line. The neutron single-particle excitation is described by a bound state of ^{8}Li + a neutron in the $1p_{1/2}$ orbital in the ground state excited to ^{8}Li + a neutron in the $1p_{3/2}$ orbital. The result is shown by the solid line. It is seen that neither proton nor neutron M1 excitation leads to an angular distribution that is similar to the measured one.

While ^{9}Li shows a large ground state quadrupole moment, -30.6 ± 0.2 mb [15] and -31.5 ± 0.5 mb [16], that moment is much smaller than ^{7,8} Li and slightly smaller than ^{11}Li, which sug- gests that there is a neutron sub-shell at N = 6. This trend is also consistent with the observed charge radius of ^{9}Li being the small- est in this isotopic chain [17]. The quadrupole moment can provide a measure of the deformation parameter (β_2), which is found to be 0.805 ± 0.005 using the moment -30.72 ± 0.18 mb obtained from a weighted average of the two measurements.

The equation

$$B(\mathrm{E2}(J_i \rightarrow J_f)) = \frac{1}{2J_i+1}\left(\frac{3ZeR_c^2\beta_2}{4\pi}\right)^2 \qquad (3)$$

can be used to find the $B(\mathrm{E2})$ value from the deformation parameter β_2 obtained from inelastic scattering. Ji is $3/2^-$ for $^9\mathrm{Li}_{gs}$ and Jf is $1/2^-$ for ^{9}Li first excited state. $R_C = \sqrt{(5/3)}\langle r^2\rangle^{1/2}$ is the mean charge radius of ^{9}Li, with Z being its atomic number. The measured root mean square charge radius of 2.245(46) fm for ^{9}Li [19] was used. Using the deformation parameter of 0.36 ± 0.05 we derive from the above relation a $B(\mathrm{E2}; 1/2^- \rightarrow 3/2^-)$ value of 2.3 ± 0.7 e^2 fm^4. Alternatively, the $B(\mathrm{E2})$ can be extracted directly from the quadrupole moment assuming a rotational model. The weighted average yields a $B(\mathrm{E2}; 1/2^- \rightarrow 3/2^-)$ value of 9.39 ± 0.11 e^2 fm^4 which characterizes the static ground state deformation. The $B(\mathrm{E2})$ extracted from inelastic scattering is significantly smaller and not compatible to that obtained from the quadrupole moment which shows that it does not describe the same deforma- tion of a ground state band.

Green's function Monte Carlo calculations have been made [18] for this transition using a Hamiltonian containing the Argonne v_{18} two-nucleon and Illinois-7 three-nucleon potential. The ground state energy is −45.2(3) MeV (Monte Carlo statistical error in parentheses), in good agreement with the experimental value of −45.34 MeV. The $1/2^-$ state is at −43.2(4) MeV, giving an exci- tation energy of 3.0(5) MeV which is consistent with the observed value within the theoretical uncertainty. The charge radius is a lit- tle small at 2.11(1) fm, and the quadrupole moment is −23(1) mb. The resulting $B(\mathrm{E2}; 1/2^- \rightarrow 3/2^-)$ is 6.8(3) e^2 fm^4. This is small compared to the value of 9.39 ± 0.11 e^2 fm^4 from the measured quadrupole moment, however it is larger than the value extracted from the analysis of the present inelastic scattering as discussed above. The corresponding $B(\mathrm{M1}; 1/2^- \rightarrow 3/2^-)$ is 3.5(1) μ^2. We note that the GFMC ground state energy, radius, and quadrupole moment are somewhat different from those discussed in Ref. [19], which were obtained with the older Illinois-2 three-nucleon potential in the Hamiltonian.

The quadrupole moment reflects only the static deformation in the equilibrium state of the nucleus, while inelastic scattering can provide information on the dynamic deformation arising from surface vibrations as well. Experimental information from both these observables can therefore lead to a complete picture on nuclear structure. The relatively small values of the deformation parameter derived from the inelastic scattering analysis in comparison to that from the quadrupole moment is perhaps due to the fact that this E2 transition is not that of a rotor with fixed intrinsic structure. Compared with the deformation in its ground state, the ^{9}Li nucleus appears to have reduced deformation when being excited to its $1/2^-$ state. The first excited state does not therefore strictly belong to the ground state band. Development of *ab initio* reaction calculations of inelastic scattering will be important for a better theoretical understanding of this.

The above observations show that the excitation of the first excited state of ^{9}Li with deuteron inelastic scattering shows the characteristic of a quadrupole excitation. We note here that the first excited state was populated in the one-neutron transfer to ^{8}Li via the ^{8}Li*(*d, p*)* reaction [12]. This suggests that the 2.69 MeV excited state in ^{9}Li might be having a mixed character of a single- particle excitation and a collective excitation. The results from this work indicate that its excitation by deuteron inelastic scattering proceeds by a relatively small value of *B(*E2*)* that is a factor of three smaller than the VMC and GFMC theoretical predictions [18]. The inelastic scattering of ^{7}Li*(*d, d^{1}*)* [20] shows that the excitation mechanism is also dominated by E2 transition. The quadrupole de- formation parameter for ^{7}Li is larger than that for ^{9}Li, which is consistent with ^{9}Li having a smaller quadrupole moment and having a possible neutron sub-shell closure at N = 6.

In summary, the elastic and inelastic scattering of ^{9}Li from deuterons measured at 5 *A* MeV using the reaccelerated beam of ^{9}Li at TRIUMF is presented. This first inelastic scattering measurement shows the angular distribution of the first excited state to be explained by a collective quadrupole excitation. The quadrupole deformation parameter derived is smaller than ^{7}Li likely due to sub-shell closure at N = 6. The deformation parameter is expected to provide some experimental guidance to future theoretical calculations for evaluating the role of the ^{9}Li excited core in binding the halo of ^{11}Li.

Acknowledgements
The authors thank the TRIUMF accelerator staff and the ISAC beam delivery group. The authors gratefully acknowledge NSERC for supporting this work. TRIUMF receives federal funding via a contribution agreement with the National Research Council, Canada. Discussions with P.D. Kunz and his kind guidance with some part of the calculations are gratefully acknowledged. The kind help of S.C. Pieper with the PTOLEMY calculations is gratefully acknowledged. The work of RBW is supported by the US Department of Energy, Office of Nuclear Physics, under contract No. DE-AC02-06CH11357. Some calculations in this work was per- formed under the auspices of the U.S. Department of Energy by Lawrence Livermore National Laboratory under Contract DE-AC52- 07NA27344.

References

[1] I. Tanihata, et al., Phys. Rev. Lett. 55 (1985) 2676.
[2] F. Barranco, et al., Eur. Phys. J. A 11 (2001) 385.
[3] I. Tanihata, et al., Phys. Rev. Lett. 100 (2008) 192502.
[4] G. Potel, et al., Phys. Rev. Lett. 105 (2010) 172502.
[5] P.G. Young, et al., Phys. Rev. C 4 (1971) 1597.
[6] F. Ajzenberg-Selove, et al., Phys. Rev. 17 (1978) 1283.
[7] D.R. Tilley, et al., Nucl. Phys. A 745 (2004) 155.
[8] R.B. Weisenmiller, et al., Nucl. Phys. A 280 (1977) 217.
[9] N.A.F.M. Poppelier, et al., Phys. Lett. B 157 (1985) 120.
[10] S.C. Pieper, et al., Phys. Rev. C 66 (2002) 044310.
[11] P. Navratil, Phys. Rev. C 70 (2004) 054324.
[12] A.H. Wuosmaa, et al., Phys. Rev. Lett. 94 (2005) 082502. [13] P.D. Kunz, http://spot.colorado.edu/~kunz/DWBA.html. [14] I.J. Thompson, Comput. Phys. Rep. 7 (1988) 167.
[15] R. Neugart, et al., Phys. Rev. Lett. 101 (2008) 132502.
[16] A. Voss, et al., J. Phys. G 38 (2011) 075102.
[17] R. Sänchez, et al., Phys. Rev. Lett. 96 (2006) 033002.
[18] S. Pastore, S.C. Pieper, R. Schiavilla, R.B. Wiringa, Phys. Rev. C, submitted for publication, arXiv:1212.3375v2 [nucl-th].
[19] W. Nörtershäuser, et al., Phys. Rev. C 84 (2011) 024307.
[20] S. Matsuki, et al., J. Phys. Soc. Jpn. 26 (1969) 1344.